Contrib Mineral Petrol (2007) 153:159–175
DOI 10.1007/s00410-006-0138-8

ORIGINAL PAPER

Fast diffusion along mobile grain boundaries in calcite

Andrew McCaig · Stephen J. Covey-Crump · Walid Ben Ismaïl · Geoffrey E. Lloyd

Received: 7 September 2005 / Accepted: 17 August 2006 / Published online: 23 September 2006
© Springer-Verlag 2006

Abstract Experimental measurements of grain boundary diffusion are usually conducted on static boundaries, despite the fact that grain boundaries deep in the Earth are frequently mobile. In order to explore the possible effect of boundary mobility on grain boundary diffusion rates we have measured the uptake of ^{44}Ca from a layer of ^{44}Ca-enriched calcite powder during the static recrystallization of a single crystal of calcite at 900°C. A region about 500 μm wide adjacent to the powder layer is heterogeneously enriched in ^{44}Ca, and complex zoning patterns, including sharp steps in composition and continuous increases and decreases in ^{44}Ca content, are developed. In metamorphic rocks, these would normally be interpreted in terms of changes in pressure or temperature, Rayleigh fractionation, or episodic fluid infiltration. These explanations cannot apply to our experiments, and instead the zoning patterns are interpreted as being due to variations in grain boundary migration rate. We have applied an analytical model which allows the product of grain boundary diffusion coefficient and grain boundary width ($D_{GB}\delta$) to be calculated from the grain boundary migration rate and the compositional gradient away from the powder layer. The value of $D_{GB}\delta$ in the mobile grain boundaries is at least five orders of magnitude greater than the published value for static boundaries under the same conditions. In order to allow the scale of chemical equilibrium (and hence textural evolution) to be predicted under both experimental and geological conditions, we present quantitative diffusion-regime maps for static and mobile boundaries in calcite, using both published values and our new values for grain boundary diffusion in mobile boundaries. Enhanced diffusion in mobile boundaries has wide implications for the high temperature rheology of Earth materials, for geochronology, and for interpretations of the length- and time-scales of chemical mass-transport. Moreover, zones of anomalously high electrical conductivity in the crust and mantle could be regions undergoing recrystallization such as active shear zones, rather than regions of anomalous mineralogy, water- or melt-content as is generally suggested.

Communicated by T.L. Grove.

A. McCaig (✉) · G. E. Lloyd
Institute of Geophysics and Tectonics, School of Earth and Environment, University of Leeds, Leeds LS2 9JT, UK
e-mail: a.mccaig@earth.leeds.ac.uk

S. J. Covey-Crump · W. Ben Ismaïl
School of Earth, Atmospheric, and Environmental Sciences, University of Manchester, Williamson Building, Oxford Road, Manchester M13 9PL, UK

Introduction

Grain boundaries exert a considerable influence on the physical properties of polycrystalline materials (Sutton and Balluffi 1995). Grain boundary diffusion is generally several orders of magnitude faster than diffusion through mineral lattices (Poirier 1985; Farver and Yund 1996; Mishin et al. 1997; Carlson 2002), and this fact is particularly important when considering:

1. the rate-competitiveness of those high temperature deformation processes which are accommodated by grain boundary diffusion (Poirier 1985; McCaig and Knipe 1990; Knipe and McCaig 1994; Langdon 1994; Mukherjee 2002),

2. processes leading to chemical homogenization in the crust and mantle (Eiler et al. 1992; Lewis et al. 1998; Steefel and Lichtner 1998),
3. metamorphic and diagenetic reactions (Carlson 2002; Putnis 2002), and
4. the interpretation of geochronological data (Freeman et al. 1997).

Diffusion along migrating boundaries can lead to complex compositional zoning patterns (McCaig and Knipe 1990; Yund and Tullis 1991; Knipe and McCaig 1994), and can itself be a driving force for grain boundary migration (Hay and Evans 1987). Moreover, recent experiments suggest that cation diffusion through grain boundaries is the dominant mechanism of electrical conductivity in fine-grained dry olivine (ten Grotenhuis et al. 2004), with important implications for conductivity anomalies in the mantle.

Modelling diffusive mass transfer within the Earth depends on the quality and relevance of experimental data. In grain boundaries it is generally only possible to measure the product $D_{GB}\delta$, where D_{GB} is the grain boundary diffusion coefficient, and δ is the effective grain boundary width (e.g. Mishin et al. 1997). Measurements of this product in minerals have invariably been made on static grain boundaries, and the question of whether such experimental data can be applied to situations where boundaries are moving has not been considered.

Experimental data on grain boundary diffusion are presently interpreted using some variant of the Fisher model (Fisher 1951). This solves the diffusion penetration relationship for diffusion from a constant-composition free surface into a semi-infinite medium containing a thin slab of high diffusivity material (representing the grain boundary) oriented normal to the surface (a problem analogous to the diffusion of heat along a thin copper foil embedded in cork). The Fisher model for a stationary boundary was adapted by Mishin and Razumovskii (1992) for a boundary moving parallel to the free surface. In doing so, they provided a method for calculating $D_{GB}\delta$ in mobile boundaries. However, despite the simplicity of the final equations, this model has not so far been used to estimate grain boundary diffusion coefficients. Here, we apply this model to the results of an experiment designed to investigate the uptake of isotopically labelled Ca into a recrystallizing single crystal of calcite. We find that the product $D_{GB}\delta$ for ^{44}Ca in moving boundaries is at least five orders of magnitude faster than the published value in static boundaries. Possible consequences of this result for the patterns and scale of diffusive processes in natural sytems are explored.

Experimental details

The experiment reported here was conducted on calcite, which is one of the best-studied mineral systems for diffusion, with tracer grain boundary diffusion parameters reported for both Ca and O (Farver and Yund 1996). Moreover, calcite is a material which readily recrystallizes at pressure and temperature conditions that are experimentally convenient.

The experimental sample was a right circular cylinder composed of a layer of calcite powder containing approximately 25% ^{44}Ca-enriched grains mixed with 75% ''normal'' calcite, sandwiched between thick discs of Carrara marble and single crystal calcite (Fig. 1). The ^{44}Ca-enriched calcite (98.53% ^{44}Ca compared with a natural abundance of 1.96%) was purchased from Oak Ridge National Laboratories. It had <10 ppm trace elements and a particle size of ~5 μm. The calcite powder with which it was mixed was analytic grade (99% + $CaCO_3$; Covey-Crump 1997a) with a particle size of ~2 μm. The single crystal was a core taken from an Iceland Spar rhomb, with the coring direction normal to a cleavage plane. The Iceland Spar contains a wide variety of trace components with a total concentration of <300 ppm (Covey-Crump 1997a). Immediately prior to the specimen assembly, the core was cleaved to provide a fresh surface for contact with the powder. The Carrara marble was a core taken from the same block of marble as used in the experiments reported by Rutter (1995) and Covey-Crump (1997b) which investigated the dynamic and static recrystallization kinetics of Carrara marble, respectively. This is a white, granoblastic calcite marble with <1% impurity phases, and calcite which is 99.76% pure with respect to solute impurities. The mean grain size (lineal intercept size) is 147 μm and the grain boundaries are well defined but non-planar. Most grains show some undulatory extinction, and there is a weak shape fabric, but there is no lattice-preferred orientation.

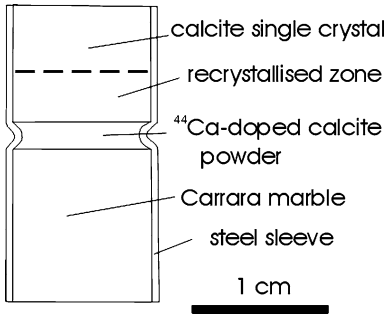

Fig. 1 Sketch longitudinal section through the experimental charge after hot pressing

The sample assembly was placed in a thin-walled iron sleeve (to keep the confining medium out of the sample) and the charge was hot isostatically pressed for 10 h at 900°C and 200 MPa confining pressure in an internally heated, argon confining medium, triaxial rock deformation apparatus (Paterson 1990). Under these conditions, fine-grained calcite powders sinter to near fully dense aggregates extremely rapidly (Covey-Crump 1997a). Given this, and the fact that the system is closed, the extent of calcite decomposition in pore spaces during the experiment can be assumed to be negligible.

After the experiment, the specimen was cut longitudinally, mounted in a block of epoxy, and syton polished before characterization using SEM electron backscatter diffraction (EBSD, e.g. Prior et al. 1999) and orientation contrast imaging (Lloyd 1987). Figure 2 shows the resulting microstructure. During the experiment, the calcite powder recrystallized to a ''foam'' texture which then underwent normal grain growth to a grain size of about 80 μm (see the bottom right part of Figs. 3a, 4). Most of the single crystal retained its original orientation with the exception of the development of thin twin lamellae (Fig. 2). However, in a layer of about 2 mm wide immediately adjacent to the powder layer, the single crystal statically recrystallized to a grain size of 100–1,000 μm (Figs. 2, 3a). The driving force for this recrystallization was the strain energy introduced into the single crystal during the initial pressurization of the charge as the powder layer compacted. There were no noticeable microstructural changes in the Carrara marble layer, which retained its initial grain size of about 150 μm. The behaviour of all three layers is in good agreement with that observed in other investigations of the static recrystallization and normal grain growth kinetics of calcite (Covey-Crump 1997a, b).

The specimen was gold coated and analysed for calcium isotopes using the Cameca ims4f ion probe at the University of Edinburgh. Images (Figs. 3, 4) were produced by collecting a map of raw counts of both ^{44}Ca and ^{40}Ca, and then using image manipulation software on the ion probe to create a new image of ^{44}Ca/(^{44}Ca + ^{40}Ca). This procedure removes bands of higher intensity caused by image overlaps and previous ion probe traces, and gives a brightness level approximating to the percent of ^{44}Ca within a particular image (minor isotopes ^{42}Ca, ^{43}Ca, and ^{48}Ca were not recorded in the mapping). Note that each image was finally converted to Tiff format before assembling montages, and in this stage equalization performed by the software means that the intensities cannot be compared directly from image to image; intensities have also been altered when stitching the images together. In the case of the profiles (Fig. 3), percentage of ^{44}Ca is derived from the raw counts by percentage of ^{44}Ca = 100 ^{44}Ca/(^{44}Ca + ^{40}Ca + ^{42}Ca + ^{43}Ca + ^{48}Ca). The profiles were measured by first burning a profile with a 4 μm step. This burned a swath of about 20 μm wide in the gold coat. Subsequently a new profile was measured along the same track with a 2 μm step, minimum apertures and zero offset, giving a significantly improved spatial resolution, estimated at 5 μm. Given the very large range in isotopic ratios in the sample (from 1.96 to 98.5% ^{44}Ca), the loss in analytical precision due to reducing the apertures was not important. In one case a profile was reconstructed from a Tiff image

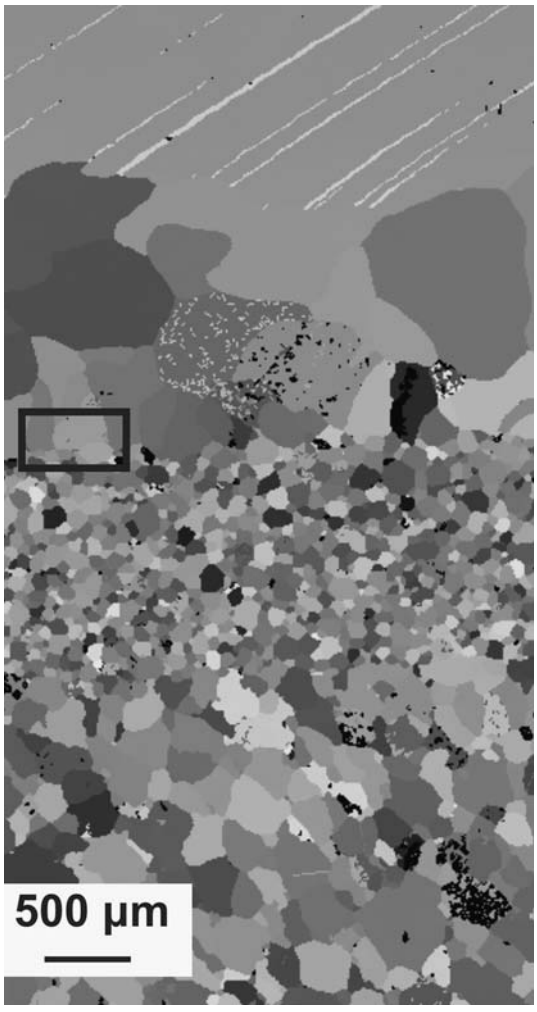

Fig. 2 EBSD map of the central part of the sample. *Greyscales* correspond to different grain orientations. Patterns were collected automatically at 10 μm intervals and processed using Channel® software. Note the twinned single crystal at the *top* of the image, the recrystallized zone *adjacent* to the fine powder layer, and Carrara marble with a weak grain shape fabric at the *bottom*. The *box* indicates the area of Fig. 3. The area of Fig. 4 extends beyond the *left-hand edge* of the EBSD map

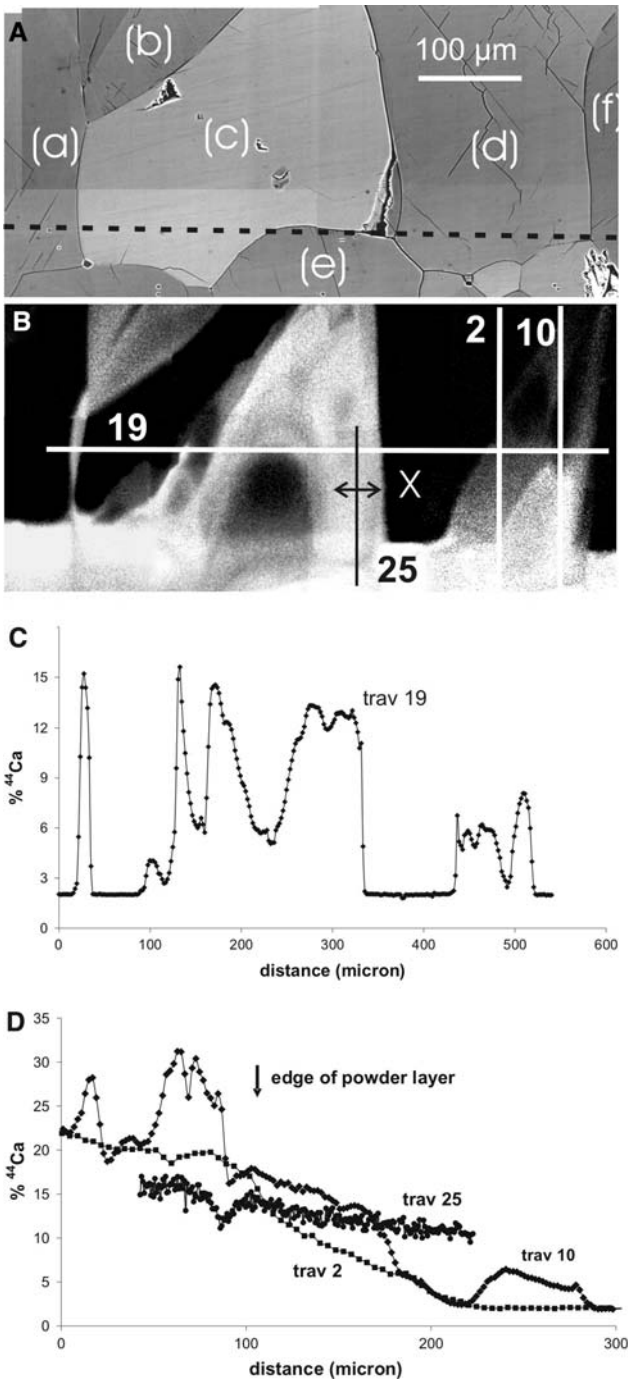

Fig. 3 **a** Orientation contrast image of the recrystallized edge of the single crystal and part of the ^{44}Ca-doped powder layer. *Contrast* in this image relates only to the orientation of calcite grains. The *dashed line* is the original position of the single crystal/powder layer interface inferred from the sharp isotopic composition contrast boundary in Fig. 3b. **b** ^{44}Ca map of the same area. Note that sharp steps in composition occur both at grain boundaries and within grains. **c** Ion probe traverse 19 as located on Fig. 3b. **d** Traverses 2, 10, and 25. Ion probe traverses 2 and 10 start *below* the image in Fig. 3b. Traverse 25 (*black line*) was reconstructed from an ion probe Tiff image using Scion® software, calibrated using spot analyses from traverses

using Scion® software (Fig. 3d, traverse 25). The absolute intensity in individual pixels was calibrated using known concentrations from tracer-free areas and a cross-cutting ion probe traverse.

Results

Ion probe images (Figs. 3b, 4b) show that significant quantities of ^{44}Ca have been incorporated into the recrystallized margin of the single crystal during grain boundary migration. Both the concentration of ^{44}Ca and the proportion of ^{44}Ca-enriched calcite decrease away from the powder layer, but ^{44}Ca contents of up to 8% were detected at over 300 μm from the original interface. Zoning patterns are complex, with both sharp steps and continuous gradients in both directions, as shown by profiles (Fig. 3c, d). Sharp steps frequently correspond to grain boundaries; others occur mid-grain, and are interpreted as former grain boundary locations. Comparison of Fig. 3a and 3b suggests that the original isotopic interface is located 30–40 μm away from the current edge of the coarse recrystallized layer, implying that new grains nucleating near the interface have grown into both the single crystal and the powder layer. The original interface is marked by a sharp step in isotopic composition not linked to current grain boundaries.

Figure 4b shows the distribution of ^{44}Ca in part of the recrystallized powder layer, while Fig. 5 shows a typical traverse across this material. It is clear that the bright, sometimes euhedral areas in Fig. 4b are relict ^{44}Ca-enriched grains which grew during the experiment, were not swept by any grain boundary, and hence preserved their initial composition. Figure 5 traverses across one such core, with peak compositions of 96% ^{44}Ca. Since the size of these enriched areas is comparable to the size of the ion beam, it is not possible to obtain an analysis which is not contaminated by adjacent less enriched material, and we believe that these cores have not been altered at all from the initial doped powder composition. Around the cores, the ^{44}Ca content of the calcite drops very rapidly and most analysis points within the powder layer are between 20 and 30% ^{44}Ca (Fig. 5). Other peaks in ^{44}Ca content within Fig. 4b are interpreted to be ^{44}Ca-enriched grains which have been swept by grain boundaries and incorporated into growing grains. Peak compositions in such cases are between 30 and 80% ^{44}Ca. It is clear that the grain growth can partially homogenize ^{44}Ca ratios within the layer, but that more than one pass of the grain boundaries is required to remove all traces of the original composition (cf. Jessell 2004).

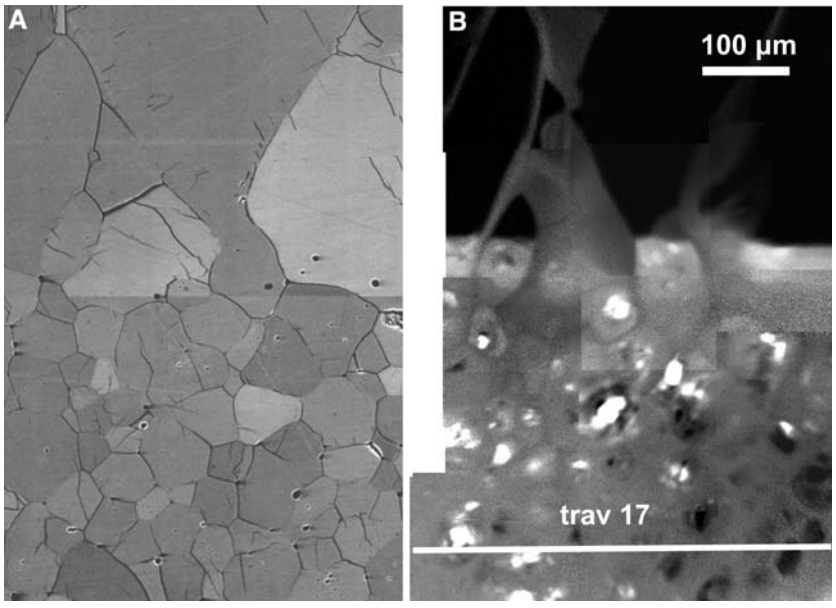

Fig. 4 **a** Orientation contrast image showing part of the fine powder layer and the interface with the recrystallized single crystal. **b** Ion probe collage of approximately the same area. Precise correlation of the images proved difficult, and *traverse 17* is also located only approximately

Model for tracer distribution in and around a moving grain boundary

Theoretical models of the diffusion of tracer along moving grain boundaries predict very different patterns of tracer distribution from those produced by diffusion along static grain boundaries (Mishin et al. 1997). Mishin and Razumovskii (1992) developed an analytical solution for the situation shown in Fig. 6, in which a migrating boundary within an initially tracer-free medium is oriented perpendicular to an interface carrying a tracer source of constant composition. They showed (Mishin and Razumovskii, 1992, Eq. 18) that provided the parameter $\gamma = Vt/(D_v t)^{0.5} > 6$, the distribution of tracer around and behind the moving boundary reaches a steady state given by:

$$C = C_1 \exp\left[-y\left(\frac{V}{D_{GB}\delta}\right)^{0.5}\right] \exp\left[-\frac{xV}{D_v} H\left(x - \frac{1}{2}\delta\right)\right] \quad (1)$$

where C_1 is the concentration at $y = 0$, V is the grain boundary migration velocity, D_v and D_{GB} are the volume and grain boundary diffusion coefficients, respectively, δ is the grain boundary width, and $H(x)$ is the Heaviside unit step function. This model is a good approximation to the situation shown in Fig. 3 where boundaries, which were oriented at a high angle to the interface with the powder layer, have migrated across the single crystal. At 900°C, D_v for Ca in calcite is 1.3×10^{-18} m^2 s^{-1} (Farver and Yund 1996). The characteristic volume diffusion distance $(D_v t)^{0.5}$ under the conditions of our experiment at $t = 10$ h is therefore expected to be 0.2 μm. Hence any variations in the

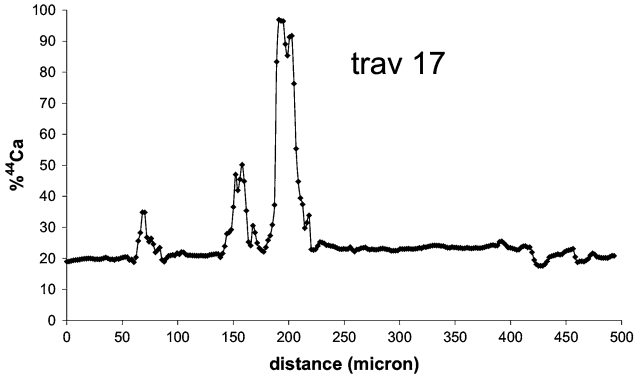

Fig. 5 *Traverse 17* in the fine powder layer. Note the ^{44}Ca-rich grain cores corresponding to the bright euhedral original powder grains in Fig. 4b. Much of the traverse has reached an approximate average composition of about 23% ^{44}Ca

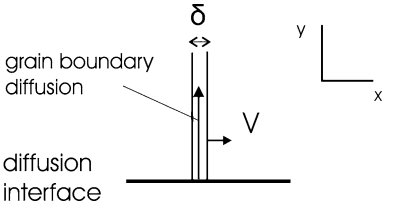

Fig. 6 The grain boundary geometry for which Mishin and Razumovskii (1992) have produced the analytical solution for tracer concentrations given in Eq. 1. δ represents the grain boundary width, and V is the grain boundary migration velocity (which is parallel to the constant composition surface). Note that with $V = 0$, the geometry is the same as used by Fisher in solving the diffusion problem for a stationary grain boundary (Fisher 1951)

^{44}Ca concentration resulting from volume diffusion are unresolvable by the ion probe in spot or traverse mode and are much less than the characteristic distance for grain boundary migration Vt. Volume diffusion can therefore be neglected in the analysis of zoning patterns. The predicted value of $D_{GB}\delta$ at 900°C is 2×10^{-21} m^3 s^{-1} (Farver and Yund 1996). Using the same authors' estimate of $\delta = 3 \times 10^{-9}$ m, the expected characteristic distance for grain boundary diffusion, under the conditions of our experiment and with $t = 10$ h, is 155 μm, although this will be considerably retarded if tracer leaks into the grains (Mishin et al. 1997). With $(D_v t)^{0.5} = 0.2$ μm at the end of the experiment, then the parameter $\gamma = Vt/(D_v t)^{0.5}$ is greater than 6 for any zone (Vt) greater than 1.2 μm wide. Hence, steady state will be achieved very quickly for any constant velocity of boundary migration which resulted in an observable zone.

Interpretation of zoning patterns

The concentration gradient away from the tracer source in the area swept by the moving boundary can be easily derived from Eq. 1:

$$\partial(\ln C)/\partial y = -(V/D_{GB}\delta)^{0.5} \quad (2)$$

Eq. 2 can be used to interpret the complex zoning patterns seen in Fig. 3b. Bright zones reflect high C (and therefore low dC/dy) and hence slow grain boundary migration, whereas dark zones reflect low C and therefore high dC/dy and hence fast grain boundary migration. It follows that the complexities of the zoning patterns can be interpreted primarily in terms of variations in grain boundary migration velocity.

For a boundary oriented at a high angle to the diffusion interface (such as that between grains (c) and (d) in Fig. 3), transverse profiles such as that numbered 19 in Fig. 3b are expected to record a constant composition if the boundary migration velocity was constant. Sharp steps in composition occur if the boundary migration velocity changed suddenly, or if the traverse crosses the final position of the migrating boundary. In the latter case the direction of boundary migration must have been towards the unenriched area, since once a grain has been enriched, tracer cannot be completely removed from it by diffusion. Continuous zoning profiles [such as the increasing ^{44}Ca content around the central dark zone in grain (c)] occur if the migration velocities changed gradually. Where boundaries migrate in a direction perpendicular to the interface, continuous changes in composition in the direction of migration may also occur even at steady state because the distance from the diffusion interface would then be changing—this may be the case for parts of profile 10. SEM EBSD analysis (Fig. 2) shows that none of the grains in the area of Fig. 3 have the orientation of the original single crystal. Tracer enriched parts of Fig. 3 have therefore been swept at least twice by grain boundaries. In some cases reversals of grain boundary migration direction appear to have occurred, for example at the boundary between grains (b) and (c).

Calculation of diffusion parameters

Equation 2 can be rearranged to allow values of $D_{GB}\delta$ to be estimated, provided that the grain boundary migration velocity is known,

$$D_{GB}\delta = V/(\partial(\ln C)/\partial y)^2 \quad (3)$$

To use this equation we must assume that a steady state was reached, that $D_{GB}\delta$ is not dependent on boundary migration velocity, and that the tracer layer is effectively a constant source of tracer. Although Eq. 2 applies to a fixed composition boundary condition, Güthoff et al. (1993) report that this equation can also be used in the case of a thin film boundary condition. Boundary conditions in our experiment in fact approximate more closely to a constant composition source than a thin film. In the tracer-enriched powder layer, although a wide range in composition from around 10 to 97% ^{44}Ca has been recorded in profiles (Fig. 5), a strong compositional mode at 20–25% ^{44}Ca is present. This compositional range was not present in the powder layer before recrystallization, and is a little lower than the mean composition of the layer as a whole (26% ^{44}Ca). Allowing for ^{44}Ca-enriched grain cores which are isolated from grain boundaries, the effective average composition of the layer as a source of tracer is about 23% ^{44}Ca. In order to calculate $\partial(\ln C)/\partial y$, we therefore assume that the recrystallizing powder layer represents a constant composition source (C_1) containing 23% ^{44}Ca, while the value in the single crystal $C_0 = 1.96\%$ ^{44}Ca. Figure 7 shows profiles 2 and 25 in Fig. 3b recast in terms of ln C' versus distance, where $C' = (C–C_0)/(C_1– C_0)$. Profile 25, which was recovered from an ion probe image and calibrated using other measured profiles, gives a gradient $\partial(\ln C')/\partial y$ of 2.9×10^3 m^{-1}. The main linear segment of the directly measured profile 2 gives a gradient of 1.5×10^4 m^{-1}. A shorter linear segment gives a gradient of 6.9×10^4 m^{-1}, but is unlikely to represent a

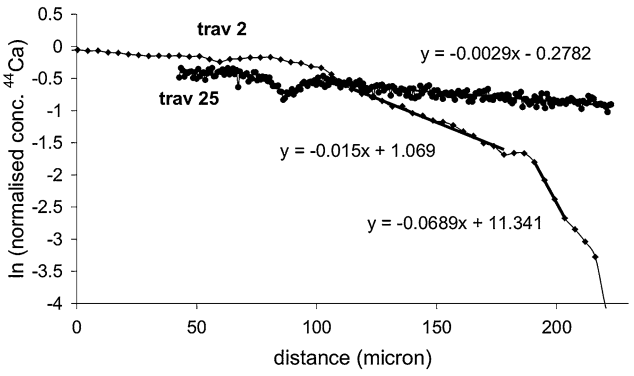

Fig. 7 Profiles 4 and 25 in Fig. 3 recast in terms of ln C'. See text for details

steady state. Since profile 2 is oblique to the zones of changing ^{44}Ca content, these are *maximum* values of the gradient parallel to the grain boundary.

Equation 3 shows that the lowest values of V that occurred during the experiment should have resulted in zones with the lowest values of $\partial(\ln C)/\partial y$. Matching the lowest *observed* value of $\partial(\ln C)/\partial y$ with the lowest *possible* value for V for a particular zone will clearly yield a minimum estimate of $D_{GB}\delta$. In our experiments, boundary velocities are unknown, but minimum velocities for particular growth zones can be estimated by dividing the width of the zone by the total time (10 h) of the experiment. For example, the width of zone X (Fig. 3b) is 50 μm, giving a *minimum* migration velocity of 1.4×10^{-9} m s^{-1}. In practice this probably underestimates velocities by at least an order of magnitude, since boundaries in the single crystal have migrated by at least 2 mm in total during the 10 h experiment. Note that Hay and Evans (1992) report maximum migration velocities of 6×10^{-9} ms^{-1} in *in-situ* experiments on chemically-induced grain boundary migration (CIGM) in calcite.

The $D_{GB}\delta$ calculated from Eq. 3 is 1.7×10^{-16} m^3 s^{-1} for profile 25 and 6×10^{-18} m^3 s^{-1} for the main linear segment in profile 2, and it is apparent from the preceding discussion that these are *minimum* values which are likely to be underestimated by at least an order of magnitude. The higher of the two values is five orders of magnitude faster than the value 2×10^{-21} m^3 s^{-1} reported by Farver and Yund (1996). We interpret this difference to reflect the difference in grain boundary diffusion rates in mobile versus static grain boundaries. However, there are other factors which may contribute to the difference which ought to be considered first:

1. Any movement of the grain boundaries in Farver and Yund's experiments would have led to an underestimate of $D_{GB}\delta$ (Mishin et al. 1997). Equation 2 can be used to calculate a gradient $\partial(\ln C)/\partial y$ for any value of V and $D_{GB}\delta$. This can then be used to calculate a new value of $D_{GB}\delta$ using the static boundary equation (Farver and Yund 1996). If boundaries moved 1 μm in a typical 18 h experiment, $D_{GB}\delta$ would be underestimated by a factor of about two. Movement by 100 μm in 18 h would lead to an underestimate by two orders of magnitude. Farver and Yund (1996) sought to avoid this problem by checking for microstructural changes using TEM, and by using pre-annealed Solnhofen limestone. This fine-grained (7 μm) limestone contains a few percent of second phase impurities which effectively render the grain boundaries immobile during isostatic heat treatments at 900°C. It is most unlikely that boundaries moved by more than 1 μm during their experiments without leaving a microstructural signature, and hence this cannot explain the discrepancy between our results. Moreover, since grain boundary mobility is strongly temperature dependent, inaccuracies in estimates of $D_{GB}\delta$ from this source would be apparent in Arrhenius plots, and hence it is unlikely that the estimates of Farver and Yund of this parameter were orders of magnitude in error.
2. Anything which affects grain boundary structure potentially affects grain boundary diffusion rates (Sutton and Balluffi 1995). This could include solute impurities contained within the grain boundary, and lattice preferred orientation. In many materials, the solutes segregate to grain boundaries such that the equilibrium concentration in the boundary is greater than in the lattice. The presence of solutes can reduce both the rate of grain boundary migration and grain boundary diffusion. If a boundary migrates fast enough to escape its solute cloud, a step change in migration rate and diffusion rate could occur (Sutton and Balluffi 1995), and this might explain differences in measured diffusion rates between stationary and mobile boundaries. However, where solute impurity effects have been quantified, the difference in grain boundary diffusion rate was only a factor of two to four (Surholt and Herzig, 1997). Furthermore, the effect is greatest in extremely pure materials, rather than the natural materials used both by ourselves and Farver and Yund (1996). Although solute effects on grain boundaries in geological materials deserve further study, it seems unlikely that they could account for more than five orders of magnitude difference in diffusion rate between experiments on comparable materials.

Effects of lattice-preferred orientation could be considerable for specific boundary types, for example coherent tilt boundaries where the boundary consists of a set of parallel edge dislocations (Sutton and Balluffi 1995). However, in the recrystallized single crystals in our experiments a wide variety of both lattice and boundary orientations occur (Fig. 2), and most boundaries must be incoherent. A similar range in boundary mismatches must have occurred in the materials used by Farver and Yund (1996), so it seems unlikely that crystallographic effects could explain the discrepancy between the experimental results.

3. The presence of water in the experimental charges is potentially significant in influencing grain boundary diffusion rates. Large differences in oxygen volume diffusion rates have been reported between dry and wet conditions (Farver 1994). These differences were attributed to molecular water being the dominant diffusion species. Calcium diffusion in both the lattice and grain boundaries has only been studied in nominally dry conditions (Farver and Yund 1996), and oxygen grain boundary diffusion in calcite has only been studied under hydrothermal conditions (Farver and Yund 1998). However, Kronenburg et al. (1984) found no difference in carbon diffusion rates between dry and wet conditions, and it is unlikely that molecular water would significantly enhance rates of calcium diffusion. Our experiments were nominally dry, but the calcite powders would have contained adsorbed water from the atmosphere. The samples of Farver and Yund would have also contained water given off by the dehydration of hydrous impurity phases in the Solnhofen limestone. Consequently, it is difficult to see how water in the grain boundaries could account for the difference in diffusion rates, although a more systematic study of grain boundary diffusion rates under dry and hydrothermal conditions is clearly desirable.

Discussion

Quantification of diffusion regimes

The concept of diffusion regimes has been widely applied in the Materials literature (Hart 1976; Cahn and Balluffi 1979; Mishin and Razumovskii 1992; Balluffi et al. 2005), and more rarely in Earth Sciences (Evans et al. 1986), but such regimes have rarely been quantified. Here, we take the opportunity to make a quantitative analysis of diffusion regimes and distances, including a treatment of mobile grain boundaries, for polycrystalline calcite. This is possible because for calcite, data not only on grain boundary and volume diffusion, but also on grain boundary migration rates as a function of temperature and driving force, are now available.

Qualitative treatment

Figure 8 shows the classic treatment of diffusion regimes in stationary and mobile boundaries (Cahn and Balluffi 1979). On the left side of the diagram are the regimes for stationary boundaries as defined by Harrison (1961). When the characteristic distance for lattice diffusion, $(D_v t)^{0.5} > d$, where d is the grain size, the A-regime prevails. Diffusion occurs in both the lattice and the grain boundaries, and an effective diffusion coefficient can be defined (Balluffi et al. 2005) as:

$$D_{\text{eff}} = D_v + (3\delta/d)D_{\text{GB}} \tag{4}$$

The factor $(3\delta/d)$ is the approximate ratio of atomic sites in grain boundaries to those in the lattice. If

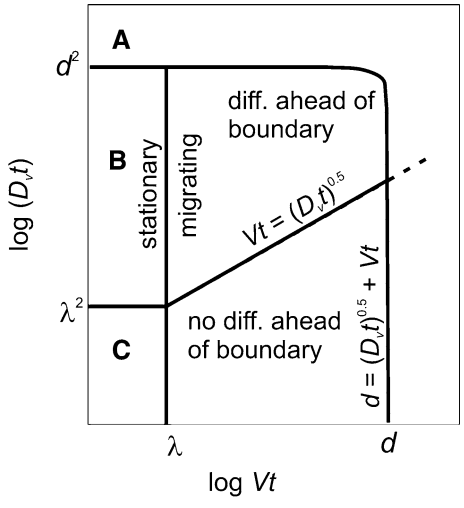

Fig. 8 Diffusion regimes for stationary and moving boundaries (Cahn and Balluffi 1979; Balluffi et al. 2005). *A*, *B* and *C* represent the regimes for stationary boundaries of Harrison (1961). The *A*-regime occurs when the characteristic distance for volume diffusion, $(D_v t)^{0.5}$, exceeds the grain size d. The *C*-regime involves no diffusion within crystals so $(D_v t)^{0.5} < \lambda$, where λ is the interatomic spacing. Boundaries can be considered mobile when the characteristic distance for migration, $Vt > \lambda$. For mobile boundaries the *A*-regime exists where $Vt > d$. Within the regime of moving boundaries, a further subdivision can be made where $Vt > (D_v t)^{0.5}$, such that no lattice diffusion occurs ahead of the moving boundaries

$(D_v t)^{0.5}$ is smaller than the atomic spacing λ, the C-regime prevails, with no lattice diffusion, although diffusion may still occur along grain boundaries. Most experiments on grain boundary diffusion are carried out in the B-regime, where diffusion occurs in both grain boundaries and the adjoining lattice, with grain centres being unaffected.

Boundaries can be considered to be migrating when $Vt > \lambda$. The A-regime for migrating boundaries occurs when $Vt > d$. Under these conditions, every atom is visited by several boundaries, and an effective diffusion coefficient can be estimated using Eq. 4 even if D_v is essentially zero (Cahn and Balluffi 1979; Balluffi et al. 2005). The migrating boundary field is further divided into a region where volume diffusion occurs in front of the migrating boundary and another where it can be neglected. This diffusion ahead of the boundary is expressed by the second exponential in Eq. 1. It is noteworthy that any system will begin at the origin in Fig. 8, and end up in the A-regime if the time elapsed is long enough.

Quantitative treatment: static boundaries

Farver and Yund (1996) used a relationship similar to Eq. 4 to discuss the scale of diffusive mass transfer under various conditions, comparing this with natural datasets. However, they did not consider moving boundaries, and did not attempt to quantify the boundary between the A- and B-regimes. Strictly speaking, whole-rock data can only be interpreted using Eq. 4 in the A-regime.

In their work on diffusion-induced grain boundary migration, Evans et al. (1986) represented Fig. 8 in ln (time) versus $1/T$ space, which is much more useful for considering geological processes. Only a qualitative treatment was possible at that time. Quantitative treatment requires not only knowledge of volume and grain boundary diffusion coefficients, but also an estimate of grain boundary migration velocity as a function of temperature and driving force.

In this space, the boundary between the A- and B-regimes for static boundaries is given by the condition $(D_v t)^{0.5} = d$ in which $D_v = D_{vo}\exp(-H_v/RT)$. On Fig. 9a this boundary is shown for calcium diffusion in calcite at a range of grain sizes using the values of Farver and Yund (1996), $D_{vo} = 0.13$ m^2 s^{-1}, and $H_v = 382$ kJ mol^{-1}. For static grain boundaries at a temperature of 700°C, the A-regime is reached after about 5,000 years for a grain size of 10 μm, and after about 10 million years for a grain size of 1 mm. It is unlikely to be reached at <500°C on geological timescales, a fact reflected in the common preservation of chemical zoning in calcite at medium grades of metamorphism.

Quantitative treatment: mobile boundaries

Calculation of the A-regime boundary for mobile boundaries, where $Vt = d$, requires grain boundary migration rates to be estimated. Driving forces for grain boundary migration include grain surface energy, intracrystalline strain energy, and chemical energy due to the overstepping of metamorphic reactions or due to diffusion-induced grain boundary migration (Balluffi et al. 2005). These driving forces are discussed in turn subsequently.

Normal grain growth under dry conditions Normal grain growth driven by surface energy minimization can be described by the equation:

$$d^{1/n} - d_0^{1/n} = k_0 t \exp(-H/RT) \quad (5)$$

where d is the grain size, d_0 is the grain size at the start of the growth period (i.e. t_0), t is the duration of the growth period, n is a dimensionless constant which depends only on the process controlling the growth rate, k_0 is a rate constant, H is the apparent activation enthalpy for the process controlling growth, R is the gas constant, and T is temperature (e.g. Covey-Crump 1997a). For a pure monomineralic system, $n = 0.5$.

In a detailed study of the normal grain growth kinetics of polycrystalline calcite, Covey-Crump (1997a) found that under pore-fluid absent conditions the growth kinetics were strongly influenced by residual porosity at low temperatures and at long times (relatively large grain sizes), when the driving force for further growth was relatively small. In these circumstances n can vary between 0.25 and 0.5. However, in experiments on Iceland Spar (the same material as used for the single crystal in our experiment), at short times (up to 1 day) at 706°C, the grain growth data were well described with $n = 0.5$. Using the rate constant at that temperature (see Covey-Crump 1997a Fig. 6), together with the activation enthalpy for the recrystallization of the calcite powders during the initial sintering phase of the experiments, then the normal grain growth kinetics are given by $n = 0.5$, $H = 240.5$ kJ mol^{-1} and $k_0 = 3.78 \times 10^{10}$ μm$^{1/n}$ s^{-1}.

We used these parameters to calculate the boundary migration velocity, V, as a function of temperature for a grain size of 30 μm by inserting $d = 31$ μm and $d_0 = 30$ μm into Eq. 5. The curve labelled "30 μm" on Fig. 9a shows the time required for the condition

$Vt = d$ to be reached for $d = 30$ μm as determined from these velocities. Since the growth rate at $d < 30$ μm is invariably greater than that at 30 μm, this is a maximum estimate of the time required for the A-regime to be reached. The curve labelled ''100 μm'' on Fig. 9a was determined in the same way but with V determined as a function of temperature using $d = 101$ μm and $d_0 = 100$ in Eq. 5. Use of the most sluggish calcite growth kinetics, affected by residual porosity and/or impurities, would shift the 100 μm curve upwards by 1.25 log units on Fig. 9a.

Also shown on Fig. 9a are the conditions at the end of our 10 h experiment. The powder layer grew by a process of strain energy driven recrystallization during sintering, followed by normal grain growth, with a final grain size of about 80 μm. Figure 9a shows that conditions would have been close to the A-regime/B-regime boundary for moving boundaries, but well within the B-regime for static boundaries, as confirmed by the preservation of unaltered grain cores where no grain boundary has swept through the material. An experimental duration of several years would have been required to reach the static boundary A-regime, even at a grain size of 10 μm. In areas which were swept by grain boundaries, initial isotopic heterogeneities have been largely smoothed out (Fig. 5), as expected for conditions close to the A-regime.

Figure 9a also shows curves for the condition $Vt = (D_v t)^{0.5}$, above which no volume diffusion occurs ahead of the moving boundary. These show that under conditions of normal grain growth, lattice diffusion ahead of the moving boundary is unimportant under virtually any natural or experimental conditions. This is why it is so critically important that boundaries are stationary during experiments to measure the product $D_{GB}\delta$ by standard profiling techniques, as discussed earlier (Farver and Yund 1996; Mishin et al. 1997).

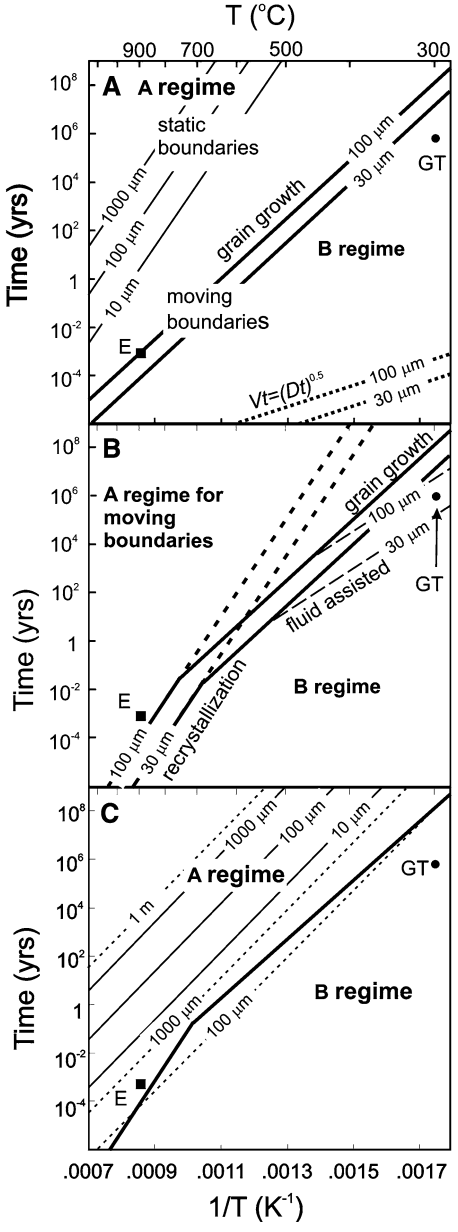

Fig. 9 Quantitative diffusion regimes for Ca in calcite. **a** ▶ Boundary between *A and B regimes* for various grain sizes, d (labels in micrometre). *Curves in upper left* are for static boundaries and represent the condition $(D_v t)^{0.5} = d$. These are also characteristic distance contours for pure lattice diffusion. *Curves in the centre* of the diagram labelled ''grain growth'' are for mobile boundaries and represent the condition $Vt = d$. Arrhenius parameters are taken from Covey-Crump (1997a) for normal grain growth of dry Iceland Spar powders (see text for details). The *curves in the bottom right* of the diagram represent the condition $Vt = (D_v t)^{0.5}$, above which there is no lattice diffusion ahead of a moving boundary, and use the same equation for Vt as the ''grain growth'' curves. Experimental conditions from this paper are labelled *E*, while approximate conditions in the Gavarnie Thrust mylonite (Knipe and McCaig 1994) are labelled *GT*. See text for details. **b** Boundary between moving boundary *A- and B-regimes* for alternative recrystallization mechanisms, with grain growth curves from Fig. 9a reproduced for comparison. *Curves* labelled ''recrystallization'' use the equation of Covey-Crump (1997b) for static recovery of Carrara marble to calculate grain boundary velocity, but with Hart's state variable replaced by the flow stress (Rutter 1995) for the given grain size in dynamic recrystallization. *Curves* labelled ''fluid assisted'' are based on the pore-fluid present grain growth experiments of Covey-Crump (1997a). **c** Characteristic diffusion distance contours (in micrometre unless otherwise stated) for moving boundaries in the *A-regime*. *Heavy line* is the *A-regime* boundary for a 100 μm grain size from diagrams **a** and **b**. *Solid contours* are characteristic distances for an effective diffusion coefficient (Balluffi et al. 2005) using the volume and grain boundary diffusion data of Farver and Yund (1996), and a grain boundary width δ of 3 nm. *Dashed lines* are characteristic distances using the enhanced value of $D_{GB}\delta$ calculated in this paper. See text for discussion

Fluid-assisted grain growth The normal grain growth kinetics of polycrystalline calcite under pore fluid present conditions was also investigated by Covey-Crump (1997a). This yielded a rather simpler dataset to interpret than the pore fluid absent experiments, and revealed a small pressure dependence of the grain growth kinetics. Incorporating the activation volume term into the activation energy at a pressure of 200 MPa yields the values $n = 0.33$, $k_0 = 5.9391 \times 10^7$ $\mu m^{1/n}$ s^{-1} and $H = 169.47$ kJ mol^{-1}. This value of n suggests that growth was controlled by diffusion in the fluid phase. These values have been used to calculate the dashed curves labelled ''fluid-assisted'' in Fig. 9b. Because of the lower activation energy, at low temperatures the A-regime for fluid assisted grain growth is reached before that for dry grain growth.

Grain boundary migration driven by intracrystalline strain energy In the single crystal in our experiments, and in many natural situations, grain boundary migration is more likely to be driven by intracrystalline strain energy than by surface energy. Indeed, surface energy is generally regarded as the smallest significant driving force for grain boundary migration (Balluffi et al. 2005). Covey-Crump (1997b) investigated the static recrystallization kinetics of previously deformed Carrara marble and found that the time taken for 50% recrystallization is given by:

$$t_{0.5} = 4.358 \times 10^{-14} \exp(-0.0308\sigma*) \exp(392400/RT) \quad (6)$$

where σ* is the mechanical state variable of Hart (1976) in MPa, which for the present purposes may be approximated by the flow stress. $t_{0.5}$ is the time taken for boundaries to migrate 75 μm, since the starting grain size in Carrara marble is ~150 μm. Equation 5 can therefore be rearranged to give the migration velocity (V) in ms^{-1}:

$$V = 7.5 \times 10^{-5}/[4.358 \times 10^{-14} \exp(-0.0308\sigma*) \exp(392400/RT] \quad (7)$$

Rutter (1995) found the following empirical, temperature-independent relationship between flow stress and recrystallized grain size for migration recrystallization from his experiments on Carrara marble:

$$\log \sigma = 2.22 + 0.37 \log d - 0.30(\log d)^2 \quad (8)$$

This relationship gives a flow stress of 58 MPa at 100 μm and 129 MPa at 30 μm. These stress values were substituted for σ* in calculating migration velocities using Eq. 7, and hence the condition $Vt = d$ for grain sizes of 100 and 30 μm (Fig. 9b, curves labelled ''recrystallization''). The activation energy of 392.4kJ mol^{-1} in Eq. 7 is very similar to the value for Ca lattice diffusion in calcite of 382 kJ mol^{-1} (Farver and Yund 1996), and so the slopes of these curves are similar to those of the curves for static boundaries in Fig. 9a. The high activation energy means that strain energy-driven recrystallization is most important at high temperatures such as those in our experiment. Figure 9b suggests that the single crystal in our experiment probably recrystallized in or near the A-regime even given the large grain size of the new grains (Fig. 2).

Stress/dynamically recrystallized grain size relationships have been reviewed by De Bresser et al. (2001), who suggest that the recrystallized grain size should track the boundary between the grain size sensitive and grain size insensitive deformation regimes, implying that this relationship should depend on temperature. We have calculated stresses using their Eq. 13 (with flow law parameter sets 6 and 8 in their Table 2). They are somewhat lower than those given by Eq. 8 at 900°C, but unrealistically high (>1,000 MPa) at temperatures <600°C, undoubtedly reflecting uncertainty in the material parameters in the relevant flow laws (De Bresser et al. 2002). Consequently, in advance of improvements in these flow laws, we have retained the more robust relationship given by Eq. 8.

Grain boundary migration driven by chemical variations Metamorphic recrystallization is driven by energy associated with the overstepping of reactions**.** This is an intrinsically more complex problem than single phase kinetics since interphase boundaries are involved, and the diffusion of components towards and away from the migrating boundary is often a rate-limiting step for the migration itself (Carlson 2002). We have not attempted to incorporate this into our quantitative treatment of diffusion regimes, although some possible consequences of our results for the interpretation of metamorphic textures are discussed subsequently.

Another important driving force for grain boundary migration is chemically induced grain boundary migration (CIGM), which has been observed experimentally in many metal alloys and also in calcite (Hillert and Purdy 1978; Chongmo and Hillert 1981; Evans et al. 1986; Hay and Evans 1987; 1992). CIGM

occurs when a component which forms a solid solution with the host mineral diffuses along the grain boundary and is incorporated into the growing grains. It has never been observed during self-diffusion of an isotopic tracer (Hay and Evans 1992; Mishin et al. 1997), and was not therefore a driving force for boundary migration in our experiments. Hay and Evans (1992) record maximum velocities for CIGM driven by Sr solid solution in calcite of 6×10^{-9} m s^{-1} at 700°C. If we compare this with velocities calculated using Eqs. 5 and 7 at the same temperature, it is about two orders of magnitude faster than either the normal grain growth rate at 30 μm, or strain energy driven migration at 128 MPa flow stress. It is clear that if CIGM occurs in nature, the A-regime for moving boundaries will be reached quite easily. One interesting observation is that a commonly advanced mechanism for driving CIGM is coherency strain (Hay and Evans 1992), in which the tracer is absorbed into the lattice ahead of the migrating boundary, creating a volumetrically strained region into which the boundary migrates. Using $D_v = 3.7 \times 10^{-22}$ at 700°C (Farver and Yund 1996) and $V = 6 \times 10^{-9}$ m s^{-1}, $Vt = (D_v t)^{0.5}$ after only 10^{-5} s. In this time, only 6×10^{-14} m of lattice diffusion could occur, far less than an atomic spacing. Under the experimental conditions of Hay and Evans (1992), it seems very unlikely that diffusion ahead of the migrating boundary could possibly drive CIGM, unless it occurred by some much faster mechanism.

Characteristic distances for diffusion in the migrating boundary A-regime

Figure 9c shows characteristic distance contours in the A-regime (solid lines) calculated using the effective diffusion coefficient from Eq. 4 and the data of Farver and Yund (1996). When compared with characteristic distances for pure lattice diffusion (the static grain boundary A-regime boundaries in Fig. 9a), it is clear how much grain boundary migration aids chemical redistribution, particularly at lower temperatures. However, only 1–5 μm of diffusion is predicted under the experimental conditions, which is clearly far less than that has occurred. When our new enhanced value of $D_{GB}\delta$ in mobile boundaries is used (dashed lines), the predicted diffusion distance is between 100 and 1,000 μm, in accordance with the observations. This supports our findings using a different method of estimating D_{GB}. The enhanced diffusion contours show that under lower crustal conditions, effective diffusion distances >1 m could be achieved in relatively short geological timescales in shear zones undergoing dynamic recrystallization.

Furthermore shown in Fig. 9 are the approximate conditions for recrystallization (~300°C, 1 million years) in carbonate mylonites beneath the Gavarnie Thrust in the Pyrenees (McCaig et al. 1995). These mylonites contain microzoning patterns within dynamically recrystallized calcite with an average grain size of 30 μm (Knipe and McCaig 1994). These have been interpreted to reflect introduction of a chemical anomaly in an advecting fluid followed by redistribution by grain boundary diffusion and incorporation of the anomaly into growing grains. Redistribution by diffusion must have occurred on a length scale of centimetres to metres, but without homogenization by volume diffusion. This suggests that the sample was in the upper B-regime or the boundary migration A-regime. Inspection of Fig. 9 suggests that these conditions could have been met if grain boundary migration was fluid assisted, but that even the enhanced diffusion rates in mobile boundaries would not redistribute chemical signatures on the scale required under dry conditions, particularly since the timescale for the chemical redistribution event may have been much less than 1 million years. It is likely that diffusion occurred via a grain boundary fluid phase, the presence of which is suggested by relict porosity (Knipe and McCaig 1994).

Reasons for faster diffusion in mobile boundaries

We conclude from our experiment that the value of $D_{GB}\delta$ for Ca in calcite was at least five orders of magnitude faster in mobile grain boundaries than that was observed by Farver and Yund (1996) in static grain boundaries. As yet we have no information on the temperature dependence of this enhanced diffusion, or on whether the diffusion coefficient varies smoothly as a function of grain boundary migration rate, or is enhanced in a step-like way when a certain boundary velocity is exceeded.

The possibility that diffusion in moving grain boundaries might be much faster than in static ones has been the subject of an extended debate in the material sciences literature. Early experiments on metals investigating grain boundary diffusion by inducing discontinuous precipitation reactions and CIGM, suggested that diffusion in moving grain boundaries was indeed several orders of magnitude faster than in stationary ones (Hillert and Purdy 1978; Chongmo and Hillert 1981). However, more recent work on a wider range of metallic systems has not confirmed this conclusion (e.g. Mishin et al. 1997; Zieba 2003. Most experiments in the material sciences literature are based on migration of interphase boundaries during

discontinuous precipitation (exsolution) reactions. This necessarily involves interdiffusion of two or more species, and so the rate of migration may be controlled by the rate of diffusion in the boundary, a situation common in metamorphism (Carlson 2002). However, in our experiments boundary migration is independent of any chemical effects and so it is the effect of migration velocity on diffusion rates in the boundary, rather than vice versa, which is of interest. It is unclear whether these differences in experimental procedure could affect the results, or if the phenomenon is material specific, perhaps related to the nature of bonding.

The fact that diffusion along static grain boundaries is several orders of magnitude faster than through the crystal lattice, reflects the fact that high angle grain boundaries are highly disordered in comparison with the lattice and as such provide a more open pathway for atomic movements (Sutton and Balluffi 1995). In materials containing ionic bonds, such as calcite, charge balance effects mean that a zone of the lattice adjacent to the boundary may also contain high defect concentrations. Consequently, the fact that grain boundary diffusion is faster in migrating boundaries than in static ones may reflect differences in the grain boundary structure between the two cases. Minerals can have extremely complex grain boundary structures. For example, HRTEM studies of olivine have revealed grain boundary microstructures including nanocrystals intermediate in orientation between the two adjacent grains and surrounded by multiple dislocations (Heinemann et al. 2003). Moving boundaries may have even more complex internal structures (and hence effective width), and glide and climb of boundary dislocations could lead to enhanced rates of diffusion. In advance of a more detailed understanding of grain boundary structure in geological materials, and of the atomistic mechanisms of grain boundary diffusion in general, considerations of this matter remain poorly constrained.

Implications for the rheology of Earth materials

Grain boundary diffusion controls the rate of deformation mechanisms such as Coble creep and diffusion-accommodated grain boundary sliding. Ordinarily, grain boundary migration in the sense discussed so far in this paper is not a major part of such mechanisms. However, there are two ways in which our results may be significant in terms of deformation rate. Firstly, it is possible that during grain boundary sliding, the internal structure of boundaries is affected and faster diffusion may occur. Secondly, it has been suggested that due to feedback between grain growth and grain size reduction due to dynamic recrystallization, many rocks may actually deform under conditions transitional between grain size-sensitive diffusional creep and grain size insensitive dislocation creep (De Bresser et al. 2001; Ter Heege et al. 2002). In these circumstances, diffusional creep would be accompanied by grain boundary migration driven by intracrystalline strain energy, and diffusion rates in the mobile boundaries would be enhanced. Normally, a transition from diffusional creep to dislocation creep, for example due to grain growth, would result in a decrease in strain rate at constant stress. A positive feedback between grain boundary migration and diffusion rates would lead to a relative increase in strain rate and perhaps a wide transition zone between the two deformation mechanisms, as observed by Walker et al. (1990) in their experiments on calcite aggregates.

Implications for the interpretation of mineral zoning patterns and reaction rims

Our experiments reveal complex zoning patterns which are interpreted to result entirely from variations in mineral growth rates within a chemical gradient. In this section we examine some comparable zoning patterns in metamorphic rocks which have been attributed to variations in temperature and pressure, to Rayleigh fractionation, or to inheritance from other phases. In some cases alternative explanations for the zoning patterns are suggested based on our experiments. We are not suggesting that the previous interpretations are incorrect, merely that the effects of variable growth rate should be considered.

Recent studies of zoning patterns in metamorphic minerals have revealed a wide range of complex zoning patterns, often different for different chemical components. For example, Yang and Rivers (2001) showed that Mn and Cr zoning patterns in a single garnet can cross each other, with the Cr zoning patterns apparently being inherited from a pre-existing layering overgrown by the garnet. In contrast, concentric Mn zoning patterns are assumed to be the result of Rayleigh fractionation due to the strong partitioning of Mn into garnet, with local equilibrium maintained with the surrounding matrix at the edge of the garnet. Examples of ''overprint zoning'' are clear in our experiments, although it is pre-existing chemical inhomogeneities in a monophase system rather than a pre-existing mineralogy which is overprinted. For example, in Figs. 3 and 4, the original interface between the ^{44}Ca-enriched powder and the single crystal is preserved locally as a sharp chemical step crossing a

new recrystallized grain. These new grains replace both the original single crystal and the powder. Equation 2 implies that steps of this type will be preserved if the characteristic distance of grain boundary migration is much greater than the characteristic grain boundary diffusion distance, i.e. $Vt >> (D_{GB}t)^{0.5}$. We assume that these steps were preserved during the initial strain-driven recrystallization, probably in a few minutes. Subsequently, the boundaries migrated much more slowly, and where boundaries cut the compositional step, it was blurred giving gradients in ^{44}Ca content which can be described by Eq. 2. The dependence of overprint zoning on both grain boundary diffusion rate and growth rate was recognized by Yang and Rivers (2001), who used a parameter GL/D, where G is growth rate, L a characteristic distance, and D grain boundary diffusion rate, to describe the phenomenon. They suggested that an inner, inclusion-rich portion of a garnet with overprint zoning of Cr grew rapidly under conditions where $GL/D > 1$, while an outer part with more uniform Cr zoning grew slowly under conditions where $GL/D < 1$. This parameter is essentially the same as the parameter $Vt/(D_{GB}t)^{0.5}$ used earlier.

Other examples of ''monophase overprint zoning'' occur in the powder layer, as seen in Figs. 4 and 5. The highest ^{44}Ca contents occur in euhedral cores to calcite grains which are assumed to be nuclei inherited from the original powder. However, spikes in ^{44}Ca content of 35 and 50% also occur in traverse 17, and these appear to be ''islands'' of enrichment within larger calcite grains. These ''islands'' are reminiscent of the isolated regions of high Mn content in garnet from Harpswell Neck, Maine, observed by Spear and Daniel (1998; 2001) and Hirsch et al. (2003). These have been interpreted to be inherited from precursor Mn-rich phases, such as ilmenite, which were incorporated into the garnet. Our experiments suggest that complex zones of this type could alternatively be a combination of grain growth and recrystallization textures. In this interpretation, original small, Mn-enriched garnet grains would be incorporated into larger ones, with the original crystallographic orientation of the small grains being removed as the grain boundary swept across them. Our suggestion differs from the interpretation of the earlier authors in that we see no conflict between the original Mn concentrations being produced by growth of small garnets, and their occurrence in a single crystal. Irrespective of the origin of the chemical heterogeneity being overprinted, if recrystallization is occurring in the B-regime for a given component, then the dispersion of that component will depend on the ratio of grain boundary diffusion rate to boundary migration rate. This gives not only a first order interpretative tool when studying such microchemical features, but also a potential quantitative method of assessing grain boundary diffusion rates of various components. In the case of the Harpswell Neck garnets, components which covary with Mn must have diffused at a similar rate or slower, while components that are found at similar concentrations within and outside the anomalous areas either diffused rapidly or were present at uniform concentration before overprinting. At Harpswell Neck, unpublished trace element data apparently supports a precursor phase other than garnet for the Mn-rich areas (W. Carlson 2006, personal communication). If ilmenite was the precursor phase, as suggested by Hirsch et al. (2003), then the fact that Mn concentration does not correlate with Fe/Mg ratio means that Fe–Mg grain boundary diffusion must have been several orders of magnitude faster than Mn grain boundary diffusion at the time of garnet growth. The ratio of diffusion rates could be readily quantified using Eq. 3 if chemical gradients across the Mn-enriched regions were quantified.

We believe that variations in crystal growth rate may contribute to a variety of other zoning patterns seen in metamorphic rocks. Continuous concentric zoning was also produced in our experiments (e.g. in the core of grain (c) in Fig. 3a, seen in traverse 19). In metamorphic rocks such zoning would generally be interpreted to be due to Rayleigh fractionation, a change in metamorphic conditions, or to discontinuous changes in the minor matrix phases contributing to the reaction (Chernoff and Carlson 1999; Carlson 2002). None of these factors can be responsible for the ^{44}Ca zoning seen in our experiments. We also observe oscillatory zoning, for example, in the outer parts of grain (c) (Fig. 3). Oscillatory zoning in metamorphic minerals has been attributed to variations in fluid supply or composition (McCaig and Knipe 1990; Yardley et al. 1991; Jamtveit et al. 1993), to changes in decompression rate (Schumacher et al. 1999), or to variations in fO_2 in the grain boundary network (Sherlock and Okay 1999). Again, none of these factors can explain the oscillatory zoning seen in our experiments. We believe that growth rate variations may be a more important control on metamorphic zoning patterns than is generally recognized, within a general framework of local component-specific disequilibrium as described by Carlson (2002). In some cases, such growth rate variations may be due to a feedback between nutrient supply to the growing grain and depletion of the grain boundary network of nutrients by mineral growth. In other cases accumulation of strain energy during deformation, or periodic pinning of grain boundaries by minor phases may be

the main control on growth rate. If we add the possibility that grain boundary diffusion rates are higher in mobile boundaries, then extraction of quantitative data on rates of metamorphic reactions from zoning patterns (Carlson 2002) may be problematic.

Implications for chemical redistribution in the crust, mantle and ice sheets

If diffusion in mobile boundaries is also faster than in static boundaries in other rock-forming minerals, such as quartz and olivine, this has profound implications for many branches of Earth Sciences. Characteristic distances for diffusion [proportional to $(Dt)^{0.5}$] could be greater by more than two orders of magnitude in actively deforming zones than in rocks where no recrystallization was taking place. Grain boundary diffusion is important in the resetting of isotopic signatures during cooling, and hence for the interpretation of cooling rates from geochronological data (Eiler et al. 1992). Recrystallization is known to be an effective mechanism for isotopic resetting in shear zones (McCaig 1997; Stünitz 1998). It is normally assumed that this is because the sweeping of grain boundaries through the material reduces the need for volume diffusion, so that chemical redistribution is effectively controlled by grain boundary diffusion. This effect is obvious in our experiments. If the rate of grain boundary diffusion is also transiently increased during recrystallization, this effect would be much greater. This could affect the interpretation of diffusively spread climate signatures in ice (e.g. Johnson et al. 1997), and the extent of isotopic homogenization in the mantle. Figure 9 provides a framework for quantifying these effects in any mineral system where the appropriate data on diffusion and grain boundary migration rates are available.

Implications for conductivity anomalies in the crust and mantle

Faster diffusion of cations in mobile boundaries could have far-reaching consequences for the interpretation of conductivity anomalies in the crust and mantle (Wannamaker et al. 2002; Booker et al. 2004). These anomalies are normally, if controversially (Yardley and Valley 1997), interpreted to be zones of anomalous composition (hydrous fluid- or graphite-rich) or physical state (melt-bearing). However, recent experimental results show that electrical conductivity in fine grained olivine is controlled by grain boundary diffusion of cations, and that, provided $\sigma_{GB} >> \sigma_{GI}$ and $\delta << d$, the bulk conductivity of a material (σ_b) is given by:

$$\sigma_b = \sigma_{GI} + \sigma_{GB}\left[1 - (1 - 3\delta/d)^{2/3}\right] \quad (9)$$

where σ_b is the bulk conductivity, σ_{GI} the grain interior conductivity (set to 1 in Fig. 10), σ_{GB} the grain boundary conductivity, δ the grain boundary width, and d the grain size (ten Grotenhuis et al. 2004). Note that Eq. 4 is an approximate version of Eq. 9. Figure 10 shows the extent of this effect for both stationary and mobile grain boundaries. The curve for stationary boundaries, constructed using $\delta = 1$ nm and $\sigma_{GB}/\sigma_{GI} = 10^5$ in Eq. 9 (ten Grotenhuis, 2004, Fig. 6), shows that the bulk conductivity is only significantly enhanced for grain sizes <200 μm, and at a grain size of 1 μm bulk conductivity is enhanced by just over two orders of magnitude. The curve for mobile boundaries, constructed using $\delta = 1$ nm and $\sigma_{GB}/\sigma_{GI} = 10^{10}$ in Eq. 9 (i.e. assuming five orders of magnitude faster diffusion in moving boundaries than in static ones) shows that the bulk conductivity is significantly enhanced at all grain sizes, and is more than seven orders of magnitude higher than the within-grain conductivity at a grain size of 1 μm. Conductivity typically varies in the upper mantle by two to three orders of magnitude (Booker et al. 2004). Our data suggest that conductivities could easily be enhanced by this amount in actively recrystallizing zones, leading to the intriguing possibility that zones of active deformation, metamorphic recrystallization, or replacive phase transitions in the crust and mantle might be detectable by electrical methods.

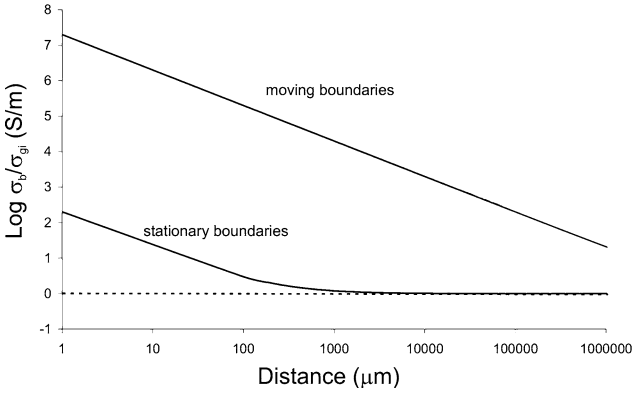

Fig. 10 Relationship between bulk conductivity (σ_b) and grain size assuming a grain boundary width of 1 nm and a grain boundary conductivity (σ_{GB}) 10^5 times greater than the grain interior permeability (σ_{GI} set to 1). *Curve* for moving boundaries based on the same equation, with σ_{GB} 10^5 times greater than the value assumed for static boundaries

Conclusions

Two important conclusions can be drawn from our study. Firstly, complex zoning patterns in metamorphic rocks could arise simply because of variations in mineral growth rate. This possibility needs to be borne in mind when interpreting zoning patterns in terms of *P–T* change, fluid infiltration, or Rayleigh fractionation. For growth rate to be an important control on mineral zoning, the characteristic distance for grain boundary movement needs to be comparable to or greater than the characteristic distance for grain boundary diffusion. The key test would be within-zone gradients in composition which can be related to local sources of mobile components, similar to the ^{44}Ca gradients seen in Fig. 2.

Secondly, grain boundary diffusion in our experiments was five orders of magnitude faster than the published value in static boundaries, and the most likely explanation is that the diffusivity in the boundaries was enhanced during migration. This result is not observed in many alloys and is almost certainly mineral specific, but it could have far-ranging consequences in petrology and geophysics. There is a clear case for further experiments both on calcite and on other mineral systems to test this possibility further and to develop the theoretical basis for the phenomenon.

Acknowledgments John Craven and Simone Käsemann are thanked for their assistance with ion probe analysis and interpretation, and Eric Condliffe for assisting with SEM analysis. Reviews by William Carlson and Timothy Grove helped to improve the manuscript, and we are grateful to the latter for suggesting the analysis of diffusion regimes. Saskia ten Grotenhuis is thanked for her comments on an earlier version of the paper. This work was supported by Royal Society Research Grant 21456 and by NERC ion probe grant IMP/162/0500. Part of it was carried out while SCC held a Royal Society University Research Fellowship

References

Balluffi RW, Allen SM, Carter CW (2005) Kinetics of materials. Wiley-Interscience, New York, 645 p

Booker JR, Favetto A, Pomposiello MC (2004) Low electrical resistivity associated with plunging of the Nazca flat slab beneath Argentina. Nature 429:399–403

Cahn JW, Balluffi RW (1979) On diffusional mass transport in polycrystals containing stationary or migrating grain boundaries. Scr Metall 13:499–502

Carlson WD (2002) Scales of disequilibrium and rates of equilibration during metamorphism. Am Miner 87:185–204

Chernoff CB, Carlson WD (1999) Disequilibrium for Ca during growth of pelitic garnet. J Met Geol 15:421–438

Chongmo L, Hillert M (1981) A metallographic study of diffusion induced grain boundary migration in the Fe–Zn system. Acta Metall 29:1949–1960

Covey-Crump SJ (1997a) The normal grain growth behaviour of nominally pure calcitic aggregates. Contrib Mineral Petrol 129:239–254

Covey-Crump SJ (1997b) The high temperature static recovery and recrystallization behaviour of cold-worked Carrara marble. J Struct Geol 19:225–241 (Erratum (1997): J Struct Geol 19: p. III)

De Bresser JHP, Ter Heege JH, Spiers CJ (2001) Grain size reduction by dynamic recrystallization: can it result in major rheological weakening? Int J Earth Sci 90:28–45

De Bresser JHP, Evans B, Renner J (2002) On estimating the strength of calcite rocks under natural conditions. In: De Meer S, Drury MR, De Bresser JHP, Pennock GM (eds) Deformation mechanisms, rheology and tectonics: current status and future perspectives. Geol Soc Lond Spec Publ 200:309–329

Eiler JM, Baumgartner LP, Valley JW (1992) Intercrystalline stable isotope diffusion: a fast grain boundary model. Contrib Mineral Petrol 12:543–557

Evans B, Hay RS, Shimuzu N (1986) Diffusion-induced grain boundary migration in calcite. Geology 14:60–63

Farver JR (1994) Oxygen self-diffusion in calcite: dependence on temperature and water fugacity. Earth Planet Sci Lett 121:575–587

Farver JR, Yund RA (1996) Volume and grain-boundary diffusion of calcium in natural and hot-pressed calcite aggregates. Contrib Mineral Petrol 123:77–91

Farver JR, Yund RA (1998) Oxygen grain boundary diffusion in natural and hot-pressed calcite aggregates. Earth Planet Sci Lett 161:189–200

Fisher JC (1951) Calculation of diffusion penetration curves for surface and grain boundary diffusion. J Appl Phys 22:74–77

Freeman SR, Inger S, Butler RWH, Cliff RA (1997) Dating deformation using Rb–Sr in white mica: greenschist facies deformation ages from the Entrelor shear zone, Italian Alps. Tectonics 16:57–76

ten Grotenhuis SM, Drury MR, Peach CJ, Spiers CJ (2004) Electrical properties of fine-grained olivine: evidence for grain boundary transport. J Geophys Res 109:B06203

Güthoff F, Mishin Y, Herzig C (1993) Self-diffusion along stationary and moving grain boundaries in α-Hf. Zeit Metall 84:584–591

Harrison LG (1961) Influence of dislocations on diffusion kinetics in solids with particular reference to the alkali halides. Trans Faraday Soc 57:1191–1199

Hart EW (1976) Constitutive equations for the nonelastic deformation of metals. J Eng Mater Technol 98:193–202

Hay RS, Evans B (1987) Chemically-induced grain boundary migration in calcite: temperature dependence, phenomenology, and possible applications to geologic systems. Contrib Mineral Petrol 97:127–141

Hay RS, Evans B (1992) The coherency strain driving force for CIGM in non-cubic crystals: comparison with in situ observations in calcite. Acta Metall Mater 40:2581–2593

Heinemann S, Wirth R, Dresen G (2003) Synthetic grain boundaries in rock-forming minerals. Eos Trans Am Geophys Union, Fall Meeting Suppl 84(46) (Abs. T41B-01)

Hillert M, Purdy GR (1978) Chemically induced grain boundary migration. Acta Metall 26:333–340

Hirsch DM, Prior DJ, Carlson WD (2003) An overgrowth model to explain multiple, dispersed high-Mn regions in the cores of garnet porphyroblasts. Am Miner 88:131–141

Jamtveit B, Wogelius RA, Fraser DG (1993) Zonation patterns of skarn garnets—records of hydrothermal system evolution. Geology 21:113–116

Jessell MW (2004) Grain growth microstructures as indicators of sample evolution, recrystallization and grain growth, pts 1 and 2. Mater Sci Forum 467–470:1051–1056

Johnson SJ, Clausen HB, Dansgaard W, Gundestrup NS, Hammer CU, Andersen U, Andersen K, Hvideberg CS, Dahl-Jensen D, Steffensen JP, Shoji H, Sveinsbjörnsdóttir AE, White J, Jouzel J, Fisher D (1997) The delta O-18 record along the Greenland Ice Core Project deep ice core and the problem of possible Eemian climatic instability. J Geophys Res 102:26397–26410

Knipe RJ, McCaig AM (1994) Microstructural and microchemical consequences of fluid flow in deforming rocks. In: Parnell J (ed) Geofluids: origin, migration and evolution of fluids in sedimentary basins. Geol Soc Lond Spec Publ 78:99–111

Kronenburg AK, Yund RA, Giletti BJ (1984) Carbon and oxygen diffusion in calcite: effects of Mn content and P_{H2O}. Phys Chem Mineral 11:101–112

Langdon TG (1994) A unified approach to grain boundary sliding in creep and plasticity. Acta Metall Mater 42:2437–2443

Lewis S, Holness MB, Graham CM (1998) Ion microprobe study of marble from Naxos, Greece: grain-scale fluid pathways and stable isotope equilibration during metamorphism. Geology 26:935–938

Lloyd GE (1987) Atomic number and crystallographic contrast images with the SEM: a review of backscattered electron techniques. Min Mag 51:3–19

McCaig AM (1997) The geochemistry of volatile fluid flow in shear zones. In: Holness M (ed) Deformation enhanced melt segregation and metamorphic fluid transport. Chapman and Hall, London, pp 227–260

McCaig AM, Knipe RJ (1990) Mass-transport mechanisms in deforming rocks: recognition using microstructural and microchemical criteria. Geology 18:824–827

McCaig AM, Wayne DM, Marshall JD, Banks DA, Henderson I, (1995). Isotopic and fluid inclusion studies of fluid movement along the Gavarnie Thrust, central Pyrenees: reaction fronts in carbonate mylonites. Am J Sci 295:309–343

Mishin YM, Razumovskii IM (1992) A model for diffusion along a moving grain boundary. Acta Metall Mater 40:839–845

Mishin YM, Herzig C, Bernadini J, Gust W (1997) Grain boundary diffusion: fundamentals to recent developments. Int Mater Rev 42:155–178

Mukherjee AK (2002) An examination of the constitutive equation for elevated temperature plasticity. Mater Sci Eng A322:1–22

Paterson MS (1990) Rock deformation experimentation. In: Duba AG, Durham WB, Handin JW, Wang HF (eds) The brittle–ductile transition in rocks (The Heard Volume). Geophys Monograph, Am Geophys Union 36:187–194

Poirier JP (1985) Creep of crystals: high temperature deformation processes in metals, ceramics and minerals. Cambridge University Press, Cambridge, 260 p

Prior DJ, Boyle AP, Brenker F, Cheadle MC, Day A, Lopez G, Peruzzo L, Potts GJ, Reddy S, Spiess R, Timms NE, Trimby P, Wheeler J, Zetterstrom L (1999) The application of electron backscatter diffraction and orientation contrast imaging in the SEM to textural problems in rocks. Am Miner 84:1741–1759

Putnis A (2002) Mineral replacement reactions: from macroscopic observations to microscopic mechanisms. Mineral Mag 66:689–708

Rutter EH (1995) Experimental study of the influence of stress, temperature, and strain on the dynamic recrystallization of Carrara marble. J Geophys Res 100:24651–24663

Schumacher R, Rotzler K, Maresch WV (1999) Subtle oscillatory zoning in garnet from regional metamorphic phyllites and mica schists, western Erzgebirge, Germany. Can Mineral 37:381–402

Sherlock SC, Okay AI (1999) Oscillatory zoned chrome lawsonite in the Tavsanli Zone, northwest Turkey. Mineral Mag 63:687–692

Spear FS, Daniel CG (1998) 3-dimensional imaging of garnet porhyroblast sizes and chemical zoning. Nucleation and growth history in the garnet zone. Geol Mater Res 1:1–43

Spear FS, Daniel CG (2001) Diffusion control of garnet growth, Harpswell Neck, Maine, USA. J Met Geol 19:179–195

Steefel CI, Lichtner PC (1998) Multicomponent reactive transport in discrete fractures: I. Controls on reaction front geometry. J Hydrol 209:186–199

Stünitz H (1998) Syndeformational recrystallization—dynamic or compositionally induced. Contrib Mineral Petrol 131:219–236

Surholt T, Herzig CHR (1997) Grain boundary self-diffusion in Cu polycrystals of different purity. Acta Mater 45:3817–3823

Sutton AP, Balluffi RW (1995) Interfaces in crystalline materials. Oxford Science Publications, New York, 819 p

Ter Heege JH, De Bresser JHP, Spiers CJ (2002) The influence of dynamic recrystallization on the grain size distribution and rheological behaviour of Carrara marble deformed in axial compression. In: De Meer S, Drury MR, De Bresser JHP, Pennock, GM (eds) Deformation mechanisms, rheology and tectonics: current status and future perspectives. Geol Soc London Spec Publ 200:331–353

Walker AN, Rutter EH, Brodie KH (1990) Experimental study of grain-size sensitive flow of synthetic, hot-pressed calcite rocks. In: Knipe RJ, Rutter EH (eds) Deformation mechanisms, rheology and tectonics. Geol Soc London Spec Publ 54:259–284

Wannamaker PE, Jiracek GR, Stodt JA, Caldwell TG, Gonzalez VM, McKnight JD, Porter AD (2002) Fluid generation and pathways beneath an active compressional orogen, the New Zealand Southern Alps, inferred from magnetotelluric data. J Geophys Res 107: art. 2117

Yang P, Rivers T (2001) Chromium and manganese zoning in pelitic garnet and kyanite: spiral, overprint, and oscillatory zoning patterns and the role of growth rate. J Met Geol 19:455–476

Yardley BWD, Valley JW (1997) The petrologic case for a dry lower crust. J Geophys Res 102:12173–12185

Yardley BWD, Rochelle CA, Barnicoat AC, Lloyd GE (1991) Oscillatory zoning in metamorphic minerals—an indicator of infiltration metasomatism. Mineral Mag 55:357–365

Yund RA, Tullis J (1991) Compositional changes of minerals associated with dynamic recrystallization. Contrib Mineral Petrol 108:346–355

Zieba P (2003) Diffusion along migrating grain boundaries. Interface Sci 11:51–58